Monte Carlo Models: *Quo Vadimus*?

Xin-Nian Wang[a*]

[a]Nuclear Science Division, MS 70-319, Lawrence Berkeley National Laboratory, Berkeley, CA 94547

Coherence, multiple scattering and the interplay between soft and hard processes are discussed. These physics phenomena are essential for understanding the nuclear dependences of rapidity density and p_T spectra in high-energy heavy-ion collisions. The RHIC data have shown the onset of hard processes and indications of high p_T spectra suppression due to parton energy loss. Within the pQCD parton model, the combination of azimuthal anisotropy (v_2) and hadron spectra suppression at large p_T can help one to determine the initial gluon density in heavy-ion collisions at RHIC.

1. Introduction

Monte Carlo models have played an important and irreplaceable role in both low and high-energy physics. First of all, they are needed to simulate the physics and detector capabilities for any proposed experiment. They are necessary to study the efficiency, acceptance corrections and background in the analyses of experimental data. They are also very useful tools for theorists to test and estimate the consequences of new physics ideas and phenomena. This is especially true for high-energy heavy-ion collisions.

In order to study the properties of the quark-gluon plasma (QGP) produced in the early stage of heavy-ion collisions and to search for evidence of the QCD phase transition, one needs to understand the whole evolution history of the collisions. Since the reaction dynamics is very complex and there is not a simple standard analytic model, one has to rely on Monte Carlo models to incorporate many aspects of strong interactions in the simulation of heavy-ion collisions. The models and parameters therein can be constrained by well-tested theories and experimental data especially in pp and pA collisions where QGP is not expected to form. They provide a baseline calculation of physical observables in the absence of new physics due to the formation of QGP. However, large uncertainties exist in extrapolating to AA collisions. Comparisons of results produced by different Monte Carlo models or by varying the model parameters are useful to provide a measure of the extrapolation uncertainties. The latest RHIC data [1–4] have proven to provide good constraints on Monte Carlo models that in turn help us to understand the reaction dynamics and the initial conditions. Finally, Monte Carlo models also serve as theoretical laboratories to test proposed signals and probes of QGP such as jet quenching [5].

*This work was supported by the Director, Office of Energy Research, Office of High Energy and Nuclear Physics, Divisions of Nuclear Physics, of the U.S. Department of Energy under Contract No. DE-AC03-76SF00098

There are many Monte Carlo models for heavy-ion collisions, reflecting the complexity of the problems. But in general they can be divided into three categories. Hadron and string based models, *e.g.*, FRITIOF [6], DPM [7], VENUS [8], RQMD [9], ARC [10], ART [11], URQMD [12], LUCIAE [13] and others, consider hadrons and Lund strings [14] as the effective degrees of freedom in strong interactions. Depending on the center-of-mass energy of a two-body collision, particles are produced through resonances and strings which hadronize according to the Lund string fragmentation model [14]. These models are adequate for particle production and rescattering in hadronic and nuclear collisions at energies around or below the CERN-SPS, in which partonic degrees of freedom are not yet important. At high energies ($\sqrt{s} > 50$ GeV), hard or semi-hard partonic scatterings become important and contribute significantly to the particle production and dominate the high p_T hadron spectra even at the CERN-SPS energy. In this case, pQCD-inspired models, *e.g.*, HIJING [15], VNI [16] NEXUS [17] and AMPT [18], are more relevant. The third class of models, such as LEXUS [19], pQCD parton model [20,21], parton cascade models [22] and hydrodynamic models [23], are not strictly event generators. But they are useful to help us to understand particle production and evolution in heavy-ion collisions, many aspects of which are difficult to simulate in an event generator.

I will not give a review of these models [24] here. Instead, I will concentrate on the parton based models and discuss the essential physics behind them. In particular, I will discuss the interplay between soft and hard processes and their different behaviors in multiple parton scattering processes. I will demonstrate the difficulties in incorporating quantum interferences in Monte Carlo models and how one can use mission specific models such as the pQCD parton model to overcome these difficulties.

2. Soft versus hard processes

Not long after the importance of minijets in both high-energy $pp(\bar{p})$ [25] and heavy-ion collisions [26] was realized, two parton-based Monte Carlo models [15,16] were developed to incorporate hard processes in high-energy heavy-ion collisions. The jet production cross section in these hard processes can be described very well by the pQCD parton model when the transverse momentum transfer p_T involved is very large. However, the pQCD parton model calculation of jet cross sections diverges when $p_T \to 0$ and the processes become non-perturbative. No theoretical model exists that can describe both the large and small p_T processes. In order to combine hard processes and non-perturbative soft processes in a Monte Carlo model, a cut-off scale p_0 in transverse momentum transfer of parton scattering is introduced that phenomenologically separates soft and hard processes. Assuming eikonalization of these processes, one can calculate the $pp(\bar{p})$ cross section in this two-component model [15],

$$\sigma_{\rm in}^{NN} = \int d^2b \left[1 - e^{-(\sigma_{\rm jet}+\sigma_{\rm soft})T_{NN}(b)}\right], \tag{1}$$

where $T_{NN}(b)$ is the nucleon-nucleon overlap function, $\sigma_{\rm soft}$ is a parameter to represent inclusive soft parton cross section and $\sigma_{\rm jet}$ is calculated from pQCD parton model,

$$\sigma_{\rm jet} = \int_{p_0^2}^{s/4} dp_T^2 dy_1 dy_2 \frac{1}{2} \sum_{a,b,c,d} x_1 x_2 f_a(x_1) f_b(x_2) \frac{d\sigma_{ab\to cd}}{d\hat{t}}. \tag{2}$$

The two parameters, p_0 and $\sigma_{\rm jet}$ in this two-component model can be fixed by the experimental data on the cross sections of $pp(\bar{p})$ collisions and the corresponding $dN_{\rm ch}/d\eta$. This is the basic principle behind HIJING [15], VNI [16] and the recent NEXUS [17]. In this two-component model, the rapidity density of charged multiplicity can be expressed as

$$\frac{dN_{\rm ch}^{NN}}{d\eta} = \langle n\rangle_{\rm soft} + \langle n\rangle_{\rm hard}\frac{\sigma_{\rm jet}^{NN}(s)}{\sigma_{\rm in}^{NN}(s)}. \tag{3}$$

In HIJING, soft particle production is modeled by a string model whose contribution to $dN_{\rm ch}/d\eta$ is almost constant. The contribution from minijet production, on the other hand, increases with energy due to the increase of the inclusive jet cross section.

To extend to nuclear collisions, one has to consider the nuclear dependences of these two components. For the soft part, the interaction is coherent and its contribution to the multiplicity should be proportional to the number of wounded nucleons. On the other hand, minijet production is approximately incoherent and proportional to the number of binary collisions, modulo the nuclear shadowing of parton distributions and jet quenching. The total charged hadronic rapidity density will acquire the form

$$\frac{1}{\langle N_{\rm part}\rangle/2}\frac{dN_{ch}^{AA}}{d\eta} = \langle n\rangle_{\rm soft} + \langle n\rangle_{\rm hard}\frac{\langle N_{\rm binary}\rangle}{\langle N_{\rm part}\rangle/2}\frac{\sigma_{\rm jet}^{AA}(s)}{\sigma_{\rm in}^{NN}}, \tag{4}$$

where $\sigma_{\rm jet}^{AA}(s)$ is the averaged inclusive jet cross section per NN collision in AA, which is generally smaller than $\sigma_{\rm jet}^{NN}$ due to nuclear shadowing of parton distributions. The energy dependence of the minijet cross section $\sigma_{\rm jet}^{AA}(s)$ in the hadronic multiplicity is then amplified by $\langle N_{\rm binary}\rangle/\langle N_{\rm part}\rangle \sim A^{1/3}$ in heavy-ion collisions relative to $pp(\bar{p})$ by the binary nature of semi-hard processes.

Shown in Fig. 1 are HIJING results of $dN_{ch}/d\eta$ per pair of participant nucleons in $pp(p\bar{p})$ and central $Au+Au$ collisions at different colliding energies as compared to experimental data. The rise of the multiplicity per participant relative to SPS is consistent with the predicted binary scaling of the hard component from pp to AA via Eq. (4) without jet quenching. Final state interaction such as jet quenching will enhance the A dependence of $dN_{ch}/d\eta$ especially at high energies.

Also shown in Fig. 1 is the result of a final-state saturation model by EKRT [29]. In this model, the pQCD growth of low p_T gluons is cut off below a saturation scale which is determined by the local saturation requirement, $dN_g/dyd^2s = p_{sat}^2/\pi$. Here dN_g/dyd^2s is the gluon rapidity density per unit transverse area. The resultant saturation scale increases with energy and $\langle N_{\rm part}\rangle$. Assuming direct proportionality between parton and the final hadron number, the energy and nuclear dependence of the total hadronic rapidity density in central $A+A$ collisions can then be estimated. As shown, the EKRT result is remarkably close to the HIJING results and is also consistent with the RHIC data.

However, a critical difference between these models is the centrality dependence of $dN_{ch}/d\eta\langle N_{\rm part}\rangle$. In the HIJING two-component model of minijet production the multiplicity per participant increases with A according to Eq.(4) while it actually *decreases* in the EKRT model with increasing A due to the saturation requirement. In order to distinguish the fixed-scale and saturation models of entropy production, the study of centrality dependence of the hadronic multiplicity per participant was proposed [31].

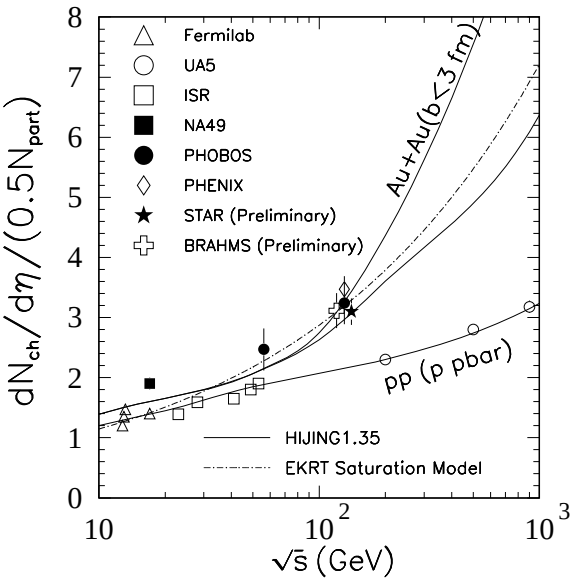

Figure 1. The RHIC data[1–4] for central Au+Au are compared to pp and $p\bar{p}$ data [27] and the NA49 $Pb+Pb$ data [28]. HIJING1.35 (solid) with (upper) and without jet quenching (lower) and EKRT (dot-dashed) predictions [29] are also shown.

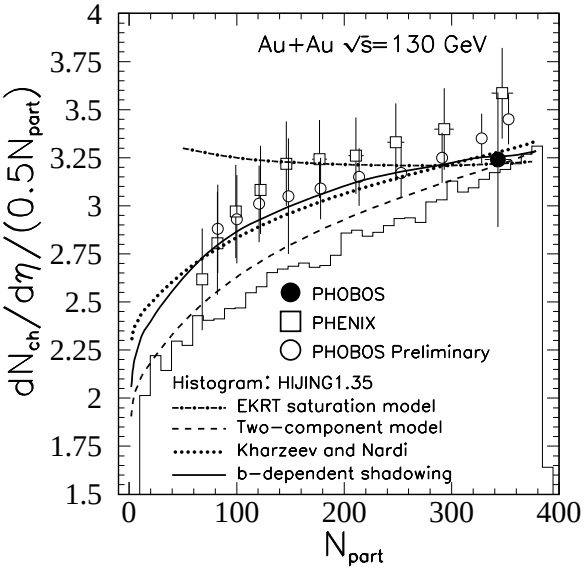

Figure 2. The RHIC data [2,3] on centrality dependence of $dN_{\rm ch}/d\eta/0.5\langle N_{\rm part}\rangle$ are compared with HIJING and EKRT [29] predictions. The two-component model in Eq. (4) with (solid) and without (dashed) b-dependence of shadowing are also shown.

Shown in Fig. 2 are the $dN_{ch}/d\eta$ per participant pair as functions of $\langle N_{\rm part}\rangle$. The EKRT model [29] has a weakly decreasing or constant dependence on centrality in semi-peripheral to central collisions. The HIJING result, on the other hand, increases monotonically with the number of binary collisions per participant $\langle N_{\rm binary}\rangle/\langle N_{\rm part}\rangle$ in an intuitive way as given in Eq.(4). The RHIC data clearly favor the the latter case. Naively, $\langle N_{\rm binary}\rangle/\langle N_{\rm part}\rangle \sim \langle N_{\rm part}\rangle^{1/3}$. The deviation from such a simple dependence in HIJING calculation might be due to a combined effect of jet quenching and dilute edges in nuclear distributions used in HIJING. Also shown as dashed line is the simple two-component model in Eq. (4) which agrees with the HIJING result. The parameters, $\langle n\rangle_{\rm soft} \approx 1.6$ and $\langle n\rangle_{\rm hard} \approx 2.2$ are determined from a fit to the measured energy dependence of $dn_{\rm ch}/d\eta$ in $pp(\bar{p})$ collisions. Another phenomenological two-component model by Kharzeev and Nardi [32], shown as the dotted line, assumed $dn^{pp}_{\rm ch}/d\eta = 2.25$ when fixing the parameters. It coincides exactly with the dashed line if $dn^{pp}_{\rm ch}/d\eta = 2.0$ is used.

The jet cross section $\sigma^{AA}_{\rm jet}$ used in the two-component model (dashed line) is calculated with nuclear shadowing of parton distributions averaged over mini-biased events. Shadowing reduces the effective jet cross section and thus minijet contribution to charged multiplicity. Without shadowing, the two-component model will over-predict the charged multiplicity in central $Au+Au$ collisions. However, parton shadowing should depend on the impact-parameter of nuclear collisions. If an impact-parameter dependent parton shadowing as described in HIJING [15] is used, the effective jet cross section $\sigma^{AA}_{\rm jet}$ should also depend on centrality. Using this b-dependent cross section in Eq. (4), one gets the solid line in Fig. 2. The RHIC data certainly favor this scenario. Such shadowing effect

is similar to the initial state saturation [30]. A phenomenological implementation of the initial state saturation is shown [32] to give a similar result as the two-component model. Another independent constraint is the rapidity dependence of $dN_{ch}/d\eta/\langle N_{part}\rangle$. PHOBOS preliminary [3] data are consistent with HIJING model.

3. Interplay between soft and hard processes

The centrality dependences of soft and hard processes not only manifest themselves in the total charged multiplicity but also in the hadron p_T spectra. Incoherent hard parton scattering should dominate the hadron spectra at high p_T while coherent soft interactions contribute mainly to the low p_T region. This leads to some nontrivial nuclear dependence of hadron p_T spectra. A good Monte Carlo model should be able to simulate this nuclear dependence.

In a schematic Glauber model of multiple parton scattering, one can calculate the produced parton spectra [33] in $p+A$ collisions:

$$\frac{E}{A}\frac{d\sigma^j_{NA}}{d^3p} \approx E\frac{d\sigma^j_{NN}}{d^3p} + \frac{9A^{1/3}}{16\pi r_0^2}\sum_i \int \frac{dx_i}{x_i} f_{i/N}(x_i)\left[\sum_k \int \frac{d^3p_k}{E_k} h^k_{iN} h^j_{kN} - (\sigma_{iN}+\sigma_{jN})h^j_{iN}\right], \quad (5)$$

where h^j_{iN} is the differential cross section for parton-nucleon scattering $i+N \to j+X$, and $f_{i/N}(x_i)$ is the parton distribution in a nucleon. The effective parton-nucleon total cross section is defined as $\sigma_{iN}(p_i) = \frac{1}{2}\sum_j \int \frac{d^3p_j}{E_j} h^j_{iN}(p_i,p_j)$ and the differential nucleon-nucleon cross section for parton production as $Ed\sigma^j_{NN}/d^3p = \sum_i \int \frac{dx_i}{x_i} f_{i/N}(x_i) h^j_{iN}(p_i,p)$. We have taken a nucleus to be a hard sphere of radius $r_A = r_0 A^{1/3}$.

In the above equation, the first term corresponds to the incoherent sum of single parton scatterings in a nucleus. The second term gives the nuclear modification of the parton spectrum due to multiple parton scattering inside a nucleus. This term contains contributions from both the double parton scattering and the negative absorptive correction. For a schematic study, let us assume that all partons are identical and the differential parton-nucleon cross sections have a simple regularized power-law form $h^j_{iN} \equiv h(p_T) = C/(p_T^2+p_0^2)^n$. The parameter p_0 can be considered as the scale separating soft and hard processes. One can then calculate the nuclear modification factor of the parton spectra,

$$R_A \equiv \frac{Ed\sigma_{NA}/d^3p}{AEd\sigma_{NN}/d^3p}, \quad (6)$$

which is shown in Fig. 3 for three different values of n as a function of p_T/p_0. Relative to the additive model of incoherent hard scattering, the spectra are enhanced at large p_T ($R_A > 1$) for hard processes due to multiple scattering. For soft processes at low p_T, the absorptive correction is large and the second term in Eq. (5) becomes negative, leading to the suppression of hadron spectra ($R_A < 1$). The transition between suppression and enhancement occurs at around the scale p_0 that separates soft and hard processes. If we analyze the hadron spectra in $pp(\bar{p})$ collisions as shown in Fig. 4, one can indeed see the two underlying components: one in power-law form that dominates spectra at high p_T and another in exponential form for low p_T hadrons. The transition between these two

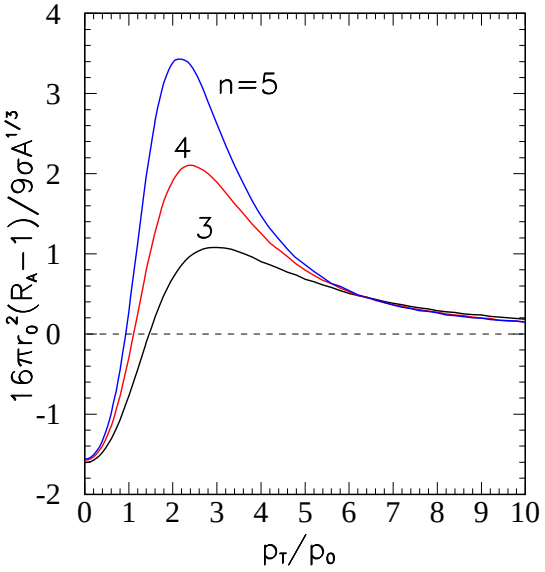

Figure 3. The nuclear modification factor in a schematic model of multiple parton scattering with a simple form of parton-nucleon cross section $1/(p_T^2+p_0^2)^n$.

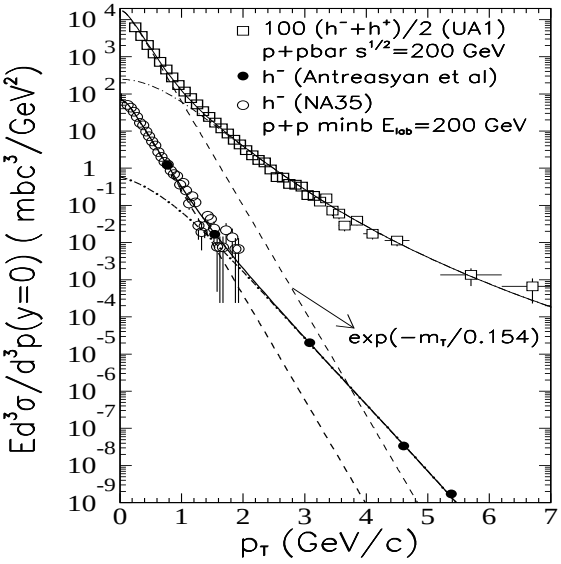

Figure 4. Experimental data [27] on hadron spectra in $pp(\bar{p})$ collisions are compared to two-component (power-law and exponential) parameterization.

components occurs at around $p_0 = 1.5 - 2$ GeV/c. Analyses of the hadron spectra in pA collisions [20,33] in terms of the nuclear modification factor indeed show such a feature in $R_A(p_T)$ and the transition scale is about $p_0 \approx 1.5$ GeV/c. These same features from initial multiple parton scattering should also appear in heavy-ion collisions if there is no final state interaction. Shown in Fig. 5 are the experimental data of central $Pb + Pb$ collisions at the CERN-SPS. These data have almost exactly the same behavior as in pA collisions at the same energy. The soft-hard transition scale is also around $p_0 \approx 1.5$ GeV/c. However, there seems to be no evidence of jet quenching at SPS [20] which would suppress the high p_T spectra.

As demonstrated in the schematic model, the unique features of the nuclear dependence of the hadron p_T spectra are consequences of the intricate quantum interference between multiple parton scattering and absorptive processes. At low p_T, the absorptive processes are dominant and they reduce the contribution of independent parton scattering. Consequently, the hadron production at low p_T appears to be coherent. The inclusive differential cross sections are only proportional to the surface area of the colliding nuclei or the number of participant nucleons. At large p_T, the destructive interference between multiple parton scattering and absorptive processes is almost complete. Hadron production processes at large p_T become incoherent. The corresponding inclusive cross sections are proportional to the volume of the colliding nuclei or the number of binary nucleon-nucleon collisions. It is difficult to simulate this quantum interference in a Monte Carlo model, especially in the transition region where both processes are important. In HIJING, the coherent soft processes are modeled by Lund-like strings whose number is proportional to the number of participant nucleons. The hard processes are treated as incoherent parton scatterings (modulo nuclear shadowing of parton distributions) that are proportional to

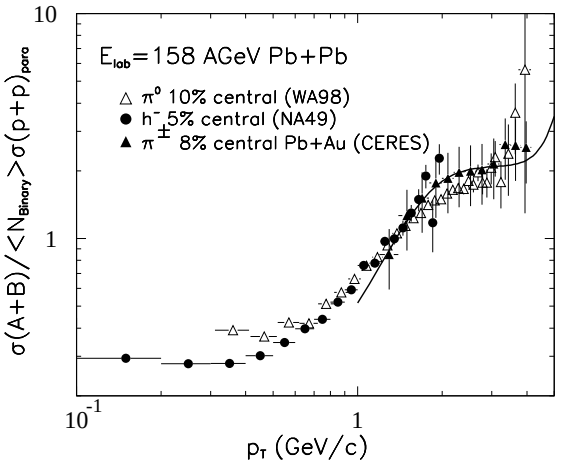

Figure 5. The nuclear modification factor for hadron spectra in central $Pb+Pb$ collisions at the CERN-SPS. The solid line is pQCD parton model calculation

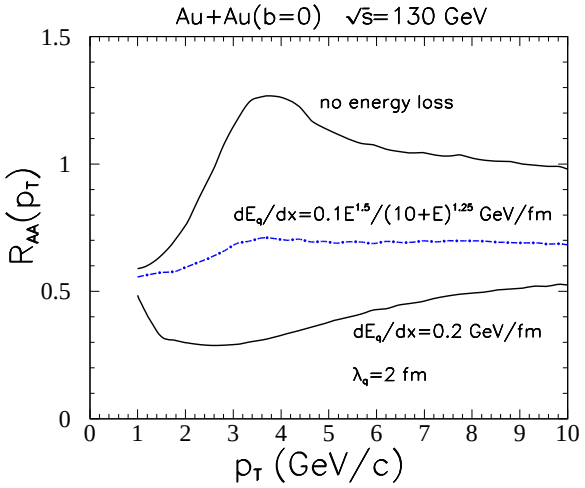

Figure 6. The nuclear modification factor for hadron spectra in central $Au+Au$ collisions at RHIC with different values of parton energy loss.

the number of binary collisions. Because of parton fragmentation, hard processes still contribute to hadron production at low p_T. However, since a p_T cut-off at $p_0 \sim 2$ GeV/c is imposed in HIJING, hard contributions to hadron production become smaller at lower p_T. Soft processes also contribute to hadron production with an exponential-like spectrum. Therefore, the resultant hadron spectra in HIJING have a smooth transition from soft to hard processes as p_T is increased [5]. However, the string fragmentation used for jets tend to suppress the p_T broadening due to multiple parton scattering. So HIJING cannot reproduce the Cronin enhancement of hadron spectra at intermediate p_T.

4. Parton model and high p_T spectra

The transition from soft to hard processes is only one example of quantum interferences one has to consider in a Monte Carlo model for high-energy heavy-ion collisions. Other effects include LPM interference effect for a propagation of an energetic parton inside a medium, coherent multiple scattering in a dense medium, and effects of chiral symmetry restoration. Implementing these phenomena correctly in a Monte Carlo model that can simulate every stage of heavy-ion collisions is very difficult, if not impossible. We can, however, resort to some mission-specific models to help us to understand the physics of some specific aspect of heavy-ion collisions. For example, hydrodynamic models [23] can help us to understand the collective phenomena in situations where cascade models become invalid because of coherent scattering in a dense medium. Parton cascade models [22] can assist us in understanding the process of parton thermalization. In the following, I will discuss the pQCD parton model [20,21], which is very useful for the study of high p_T spectra from jets. They can be used as a probe of the dense partonic matter in heavy-ion collisions.

For high p_T hadron spectra, one can essentially neglect the soft processes and only consider hadron production from hadronization of jets whose cross section can be de-

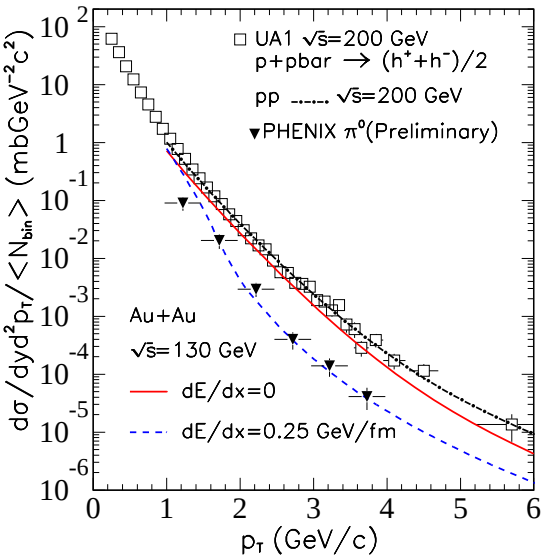

Figure 7. The preliminary π_0 spectra in central $Au + Au$ at RHIC [2] as compared to $p\bar{p}$ data [27] and parton model calculations.

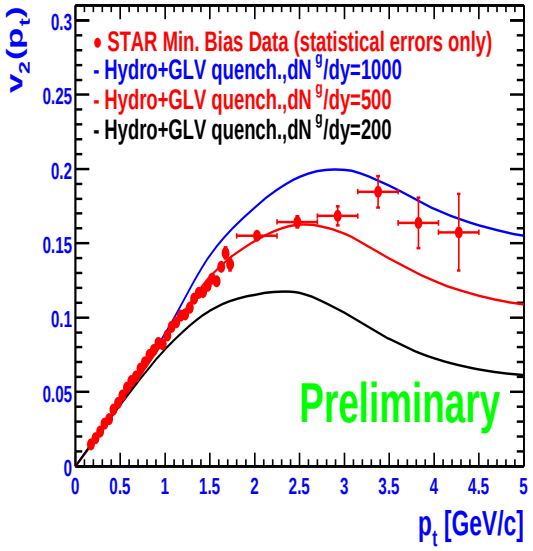

Figure 8. The hydro+parton model calculation of $v_2(p_t)$ as compared to preliminary STAR data [4].

scribed by Eq. (2). Hadron spectra in pp, pA collisions can be described well [20] within this parton model. Constrained by the existing pA data, nuclear modification of parton distributions and p_T broadening give about 10-30% increase in the p_T spectra in central $Au + Au$ collisions relative to pp without parton energy loss, as shown in Fig. 6.

Many recent theoretical studies [34] predict a large amount of energy loss by a propagating energetic parton in a dense partonic medium. In AA collisions, we model the effect of parton energy loss by the modification of parton fragmentation functions [35]. This will lead to suppression of large p_T hadrons for a non-vanishing parton energy loss relative to the null scenario. In terms of the nuclear modification factor, $R_{AB}(p_T)$ will become smaller than 1 at large p_T due to parton energy loss as shown in Fig. 6. It is also shown that the p_T dependence of $R_{AB}(p_T)$ is sensitive to the energy dependence of the parton energy loss. For more accurate determination of the energy dependence of dE/dx one should measure the high p_T hadron suppression in direct γ-tagged events [35].

Preliminary RHIC data [2,4] have indeed shown evidence of suppression of large p_T hadron spectra for the first time. This is extraordinary, given that no suppression is seen at SPS [20]. Shown in Fig. 7 are π_0 spectra [2] in central $Au + Au$ collisions as compared to pQCD parton model calculation. The model result for $p\bar{p}$ collisions at $\sqrt{s} = 200$ GeV agrees well with the UA1 data. Both the calculation and data for $Au + Au$ collisions are scaled by $\langle N_{\rm part}\rangle = \int d^2bT_{AB}(b)$ for the given centrality in order to compare to $pp(\bar{p})$ results. The preliminary data clearly show suppression of high p_T hadron spectra relative to pp. The data are consistent with the parton model calculation with an average $dE/dx \approx 0.25$ GeV/fm. I want to emphasize that this is only a phenomenological value averaged over the entire evolution history of the dense matter. It does not reveal the distance and density dependence of the dE/dx. Since the initial parton density decreases very fast

due to longitudinal expansion, such a small average dE/dx still implies very large parton energy loss in the very early stage of the dense system. Future analysis of the energy and centrality dependence [36] of the high p_T hadron suppression is important to understand the consistency between CERN-SPS and RHIC results and search for the critical initial parton density at which jet quenching becomes significant in heavy-ion collisions.

In non-central AA collisions, the total parton propagation length should depend on the azimuthal direction. Therefore, parton energy loss can also cause azimuthal anisotropy of hadron spectra at large p_T in non-central AA collisions [36]. Such azimuthal anisotropy can be calculated in the same parton model with a given parton energy loss. Shown in Fig. 8 is the calculated [36] $v_2(p_T)$ as a function of p_T as compared to STAR preliminary data [4]. The hadron spectra at low $p_T < 2$ GeV/c are assumed to be given by the hydrodynamic model and v_2 increases linearly with p_T. However, at $p_T > 2$ GeV/c, hydrodynamics will fail and v_2 should be determined by the dynamics of parton propagation in the dense medium. The parton model gives very different p_T dependence. The point where $v_2(p_T)$ deviates significantly from the hydro model signals the onset of the contribution of hard processes. As shown in the figure, v_2 at large p_T is very sensitive to dE/dx or the initial parton density. It is an alternative measurement of parton energy loss or the initial parton density. Since suppression of hadron spectra and non-vanishing v_2 at large p_T are two consequences of parton energy loss, one should be able to explain both experimental measurements and their centrality dependence with the same given parton initial density.

5. Summary

I have discussed the importance of multiple scattering, coherence and the interplay between soft and hard processes in the modeling of high-energy heavy-ion collisions. Both the nuclear dependences of rapidity density and p_T spectra have shown the onset of hard processes. The preliminary RHIC data show evidence of high p_T hadron suppression due to parton energy loss. I argued that the combination of v_2 and hadron spectra suppression will help us to determine the initial gluon density in heavy-ion collisions at RHIC.

Acknowledgement

Many results reported here are from work in collaboration with M. Gyulassy, I. Vitev and E. Wang. I also thank G. David, A. Drees, B. Jacak, P. Jacobs, F. Messer and R. Snellings for discussions.

REFERENCES

1. F. Videbaek, for BRAHMS collaboration, this proceeding.
2. W. A. Zajc; for PHENIX collab.; G. David, for PHENIX collab., this proceedding.
3. G. Roland, for PHOBOS collaboration, this proceeding.
4. J. W. Harris, for STAR collaboration, this proceeding.
5. X.-N. Wang and M. Gyulassy, Phys. Rev. Lett. **68**, 1480 (1992).
6. B. Andersson, G. Gustafson and B. Nilsson-Almqvist, Nucl. Phys. B **281**, 289 (1987); B. Nilsson-Almqvist and E. Stenlund, Comput. Phys. Commun. **43**, 387 (1987).

7. A. Capella, U. Sukhatme and J. Tran Thanh Van, Z. Phys. C **3**, 329 (1979); A. Capella, U. Sukhatme, C. Tan and J. Tran Thanh Van, Phys. Rept. **236**, 225 (1994).
8. K. Werner, Phys. Rept. **232**, 87 (1993).
9. H. Sorge, H. Stocker and W. Greiner, Annals Phys. **192**, 266 (1989).
10. Y. Pang, T. J. Schlagel and S. H. Kahana, Phys. Rev. Lett. **68**, 2743 (1992).
11. B. Li and C. M. Ko, Phys. Rev. C **52**, 2037 (1995).
12. S. A. Bass *et al.*, Prog. Part. Nucl. Phys. **41**, 225 (1998).
13. A. Tai and B. Sa, Comput. Phys. Commun. **116**, 353 (1999).
14. B. Andersson, G. Gustafson, G. Ingelman and T. Sjostrand, Phys. Rept. **97**, 31 (1983).
15. X.-N. Wang and M. Gyulassy, Phys. Rev. D **44**, 3501 (1991); M. Gyulassy and X.-N. Wang, Comput. Phys. Commun. **83**, 307 (1994) [nucl-th/9502021].
16. K. Geiger and B. Muller, Nucl. Phys. B **369**, 600 (1992); K. Geiger, Comput. Phys. Commun. **104**, 70 (1997).
17. H. J. Drescher, M. Hladik, S. Ostapchenko, T. Pierog and K. Werner, hep-ph/0007198.
18. B. Zhang, C. M. Ko, B. Li and Z. Lin, Phys. Rev. C **61**, 067901 (2000).
19. S. Jeon and J. Kapusta, Phys. Rev. C **56**, 468 (1997).
20. X.-N. Wang, Phys. Rev. C **61**, 064910 (2000) [nucl-th/9812021].
21. P. Levai, G. Papp, G. Fai and M. Gyulassy, nucl-th/0012017.
22. B. Zhang, M. Gyulassy and Y. Pang, Phys. Rev. C **58**, 1175 (1998); D. Molnar and M. Gyulassy, Phys. Rev. C **62**, 054907 (2000).
23. J. Sollfrank, P. Huovinen, M. Kataja, P. V. Ruuskanen, M. Prakash and R. Venugopalan, Phys. Rev. C **55**, 392 (1997).
24. One can download the source codes and documentations of most of these models in the OSCAR web site: http://nt3.phys.columbia.edu/OSCAR/
25. X.-N. Wang and R. C. Hwa, Phys. Rev. D **39**, 187 (1989); X.-N. Wang, Phys. Rev. D **43**, 104 (1991).
26. J. P. Blaizot and A. H. Mueller, Nucl. Phys. B **289**, 847 (1987); K. Kajantie, P. V. Landshoff and J. Lindfors, Phys. Rev. Lett. **59**, 2527 (1987); K. J. Eskola, K. Kajantie and J. Lindfors, Nucl. Phys. B **323**, 37 (1989).
27. For references on experimental data of pp and $p\bar{p}$ collisions see Refs. [31,20].
28. H. Appelshauser *et al.* [NA49 Collaboration], Phys. Rev. Lett. **82**, 2471 (1999).
29. K. J. Eskola, K. Kajantie and K. Tuominen, Phys. Lett. B **497** (2001) 39.
30. L. McLerran and R. Venugopalan, Phys. Rev. D **49**, 2233 (1994); A. Krasnitz and R. Venugopalan, Phys. Rev. Lett. **86**, 1717 (2001).
31. X.-N. Wang and M. Gyulassy, Phys. Rev. Lett. 86, 3496 (2001) [nucl-th/0008014].
32. D. Kharzeev and M. Nardi, Phys. Lett. **B507**, 121 (2001) [nucl-th/0012025].
33. E. Wang and X.-N. Wang, nucl-th/0104031.
34. M. Gyulassy and X.-N. Wang, Nucl. Phys. B **420**, 583 (1994); R. Baier, Y. L. Dokshitzer, A. H. Mueller, S. Peigne and D. Schiff, Nucl. Phys. B **484**, 265 (1997); B. G. Zakharov, JETP Lett. **65**, 615 (1997); M. Gyulassy, P. Levai and I. Vitev, Phys. Rev. Lett. **85**, 5535 (2000); U. A. Wiedemann, Nucl. Phys. B **588**, 303 (2000).
35. X.-N. Wang, Z. Huang and I. Sarcevic, Phys. Rev. Lett. **77**, 231 (1996); X.-N. Wang and Z. Huang, Phys. Rev. C **55**, 3047 (1997) [hep-ph/9701227].
36. X.-N. Wang, Phys. Rev. C **63**, 054902 (2001) [nucl-th/0009019]; M. Gyulassy, I. Vitev and X. N. Wang, Phys. Rev. Lett. **86**, 2537 (2001) [nucl-th/0012092].